Final Draft

of the original manuscript

Farhan, M.; Rudolph, T.; Noechel, U.; Yan, W.; Kratz, K.; Lendlein, A.:
Noncontinuously Responding Polymeric Actuators.
In: ACS Applied Materials and Interfaces. Vol. 9 (2017) 39, 33559 - 33564.

First published online by ACS 18.09.2017

https://dx.doi.org/10.1021/acsami.7b11316

Noncontinuously Responding Polymeric Actuators

Muhammad Farhan[1,2], Tobias Rudolph[1], Ulrich Nöchel[1], Wan Yan[1,2], Karl Kratz[1], Andreas Lendlein[1,2*]

[1] *Institute of Biomaterial Science, Helmholtz-Zentrum Geesthacht, Kantstr. 55, 14513 Teltow, Germany*

[2] *Institute of Chemistry, University of Potsdam, Karl-Liebknecht-Str. 24-25, 14476 Potsdam-Golm, Germany*

**corresponding author*: *andreas.lendlein@hzg.de*

Fax: +49 (0)3328- 352 452

Keywords: soft robotics, polymer actuators, thermo-sensitivity, shape shifting materials, crystallization behavior

Abstract

Reversible movements of current polymeric actuators stem from the continuous response to signals from a controlling unit, and subsequently cannot be interrupted without stopping or eliminating the input trigger. Here, we present actuators based on crosslinked blends of two crystallizable polymers capable of pausing their movements in a defined manner upon continuous cyclic heating and cooling. This noncontinuous actuation can be adjusted by varying the applied heating and cooling rates. The feasibility of these devices for technological applications was shown in a 140 cycle experiment of free-standing noncontinuous shape shifts, as well as by various demonstrators.

In robotics, classical actuators alternate between distinct states/shapes in response to a controlling unit. The impracticality of rigid materials, which are usually large and heavy, has made soft robotics highly desirable. Inspired by biological systems, such soft actuators are made of soft, light-weight, and flexible materials[1-3] and allow greater control and surface compatibility than their rigid counterparts.[4] Generally pneumatic methods are used to perform actuations at different length scales, however these require bulky tethered controlling units to direct the desired motions. Despite the large number of actuator systems under investigation, imitating natural movements remains a major challenge.

Unthetered soft polymeric actuators can perform relatively simple motions with degrees of freedom similar to natural organisms in one material under an external trigger. [3, 5-9] In this context different stimuli-responsive materials including: i) electro-active polymers[10-13], ii) liquid crystalline polymeric materials (LCPM)[14-17], iii) hydrogels, and iv) shape-memory actuators[18-21] have been explored. The function of soft actuators is dependent on the triggering of the respective internal driving force within the material responsible for releasing or storing energy. This leads to a corresponding volume change: in LCPMs a loss of orientation above the clearing transition temperature, in polymer hydrogels a swelling/deswelling above the lower critical solution temperature and in semicrystalline SMPs mostly solid-melt transitions. This change in volume leads to a contraction or elongantion and the actuation of the material. The trigger for this change is chosen based on the intended application of the device, and includes temperature, current, magnetic field or light. Using this approach autonomous reversible actuation between defined shapes at a variety of length scales and conditions has been realized, often with easily fabricated materials of bespoke design.

The Venus flytrap, which closes its leaves to trap its prey (and reversibly open after digestion of the prey), has generated significant interest as a natural example of a reversible actuator. However, the majority of the literature examples have been solely focused on the first closure of the leaves, and not the subsequent "locking" and "constriction" processes.[22-24] These steps are essential to ensure the successful capture of prey, release of small animals, recognition of trapped prey, and digestion.[24] Here, different individual steps take place in a noncontinuous fashion while constantly triggered. The replication of such noncontinuous natural processes could lead to new actuators/technologies which could first fix an object to perform a "sensing" step, before either a "locking" step or release. In this work we targeted a free-standing shape-shifting material with a noncontinuous response and an intermediate stable state under constant triggering conditions. For realization of such a behavior it is necessary to understand current soft actuators into more detail.

For the stress-free reversible actuation between two distinct states the response time and operating temperature range are of a high importance. Programmable materials are desired as they enable the creation of a temporary customizable shape, which can define the mode of reversible movement e.g. elongation/contraction, bending, rotation or twisting. The volumetric changes that accompany the temperature-induced transition from a crystalline to a molten state of semi-crystalline polymers can be used to create soft actuators. When the actuation domains in such materials are oriented, and can maintain their orientation while undergoing thermal transition, crystallization-induced organization of ordered macromolecules by folding of the

repeating units leads to an expansion of the polymer domain. A entropy-driven contraction occurs when an increase in temperature causes the melting of the crystalline domains. Macroscopic changes are observed as a result of these manifold nano/microlevel transitions, as has been demonstrated for bidirectional shape-memory polymer actuators.[18-21] Such polymeric actuators continuously move because of their ongoing response to repetitive temperature changes, as illustrated in Figure 1a. To realize a complex interruptive movement like that of the flytrap under continuous thermal triggering an actuator material needs to be designed, which allows nonresponse in a desired temperature interval during both heating and cooling. Such a targeted temperature response profile is shown in Figure 1b in comparison to a linear profile in Figure 1a.

Here, we use crosslinked blends of poly(ε-carpolactone) (PCL)[25] and poly(ethylene-*co*-vinyl acetate) (PEVA)[21], where the two phase-segregated regions have distinct melting (T_m) and crystallization (T_c) temperatures, and different crystallization kinetics. Here, a co-continuous phase morphology should ensure that both crytallizable actuation domains (PCL and polyethylene from PEVA) can be addressed in their individual temperature ranges independently. Covalent crosslinks are needed to provide the elasticity, which enables reversible macroscopic deformation and to increase the overall stability of the material at elevated temperatures. For actuator preparation, a blend of PCL, PEVA and dicumyl peroxide was prepared by extrusion, before crosslinked films (cPCL-PEVA) were fabricated by compression molding (Experimental, Supporting Information). Swelling experiments with toluene and chloroform provided high gel content values (G) between 90 to 95% for the cPCL-PEVAs, indicating an almost complete crosslinking reaction (Table S1). The obtained differential scanning calorimetry (DSC) thermograms for cPCL-PEVA films reflect differences in the thermal behavior of the materials. The first melting peak can be attributed to the melting of PCL crystals (T_m^{PCL}), while the second melting peak corresponds to the PE crystals (T_m^{PE}). Varying the VA content from 18 to 5 wt% caused a shift in the second melting event observed in the heating trace (Figure S1), resulting in separated or overlapping melting peaks for PCL and PEVA. The thermal and mechanical properties of the different cPCL-PEVAs are summarized in Tables S1 and S2. In our case we require two well-separated PCL and PE melting and crystallization temperatures, which was observed for cPCL-PEVA5 containing 5 wt% of VA[26]. This composition was subsequently selected for intensive investigation throughout the manuscript. DSC experiments conducted for cPCL-PEVA5 at a constant heating rate of 10 °C min^{-1} and different cooling rates of 2, 6 and 10 °C min^{-1} confirmed that the PCL crystallization behavior can be appropriately controlled (Figure S2 and Table S3). Additionally,

a cocontinuous morphology within the composite was confirmed by atomic force microscopy (AFM) and scanning electron microscopy (SEM) measurements (Figures S3 and S7 b-i). For programming, the respective specimens are stretched, twisted or bended at T_{reset} = 110 °C and cooled to 0 °C under stress to induce the formation of highly oriented crystals of both crystallizable domains. It is important to note that the programming was achieved in a one-step process and that the presented actuators can be reprogrammed to any desired other shape upon heating to T_{reset}. Figure 1c shows an illustrated manikin with a twisted arm performing rotation of a traffic sign, which enables the visualization of the reversible changes in rotation from 0 to 180° upon continuous cyclic heating or cooling from T_{low} = 25 °C to T_{high} 85 °C of the manikin in a closed heating chamber (Video S1). Determining the changes in angle of the traffic sign over the temperature range enables us to measure the actuation profile as shown in Figure 1d. Here a pronounced reversible noncontinuous (interruptive) actuation behavior is demonstrated. While a continuous change in the angle of the rotating arrow from 0 to 90° is obtained by heating from ambient temperature to 58±1 °C, in the temperature range from 59±1 °C to 70±1 °C the upright position of the traffic sign arrow remains frozen at 90°, indicating the non-response heating interval. At temperatures above 70 °C a continuous change in angle from 90° to 180° is observed. During cooling the nonresponse temperature interval ranges from 57±1 °C to 38±1 °C. The respective image series of the manikin demonstrator are displayed in Figure 1e.

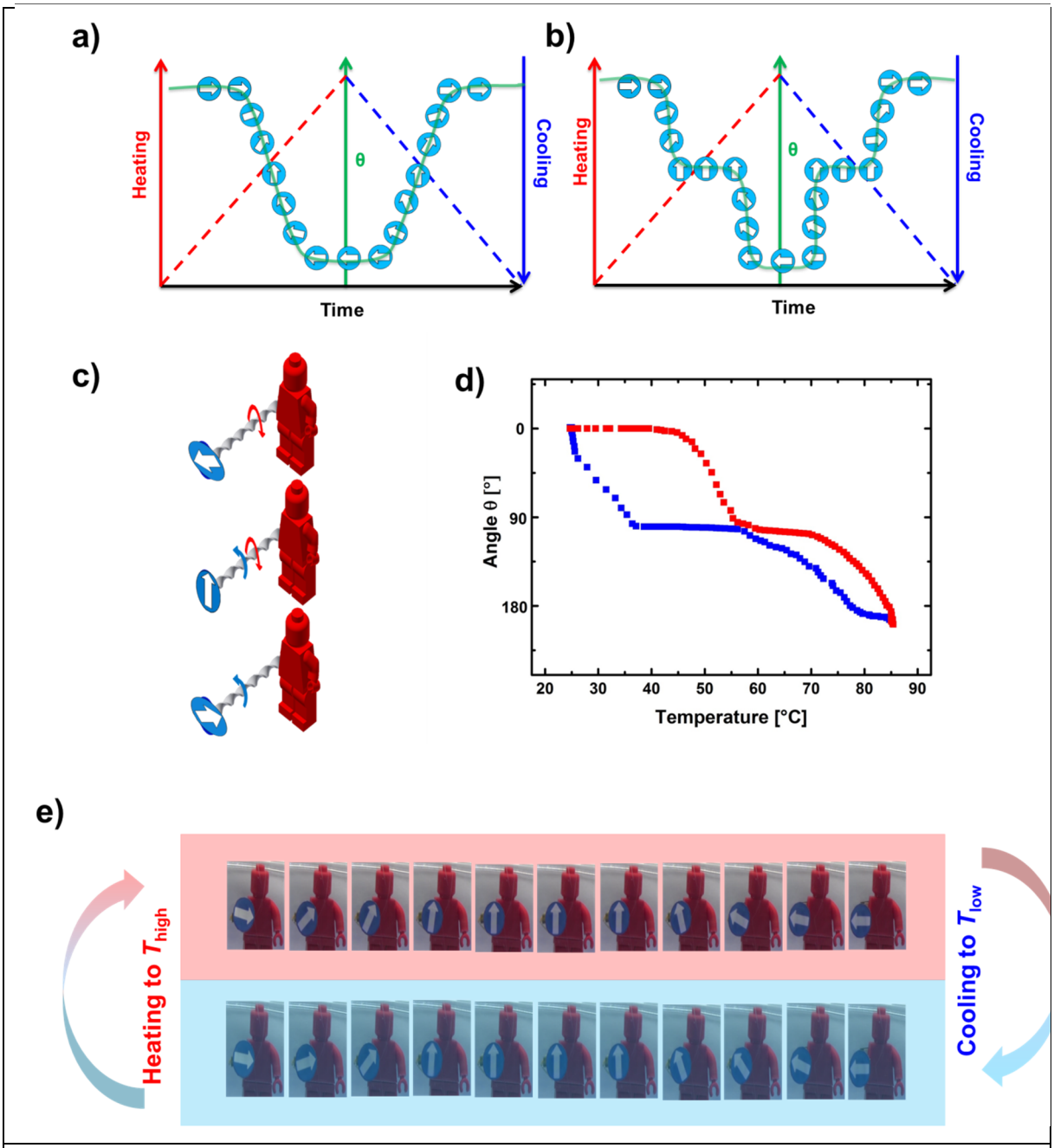

Figure 1: a) Schematic representation of time dependent shape shifts (rotations, θ) upon constant heating and cooling for continuous and **b)** noncontinuous response under constant heating and cooling. **c)** Scheme for traffic manikin having a traffic sign arrow mounted on his twisted actuator polymer arm as an example for non-continuous actuation. **d)** Change in angle of traffic sign arrow as function of temperature determined from the traffic manikin actuation video and **e)** picture series of second heating and cooling cycle taken from the video.

For a more detailed quantification of the interruptive actuation behavior of cPCL-PEVA5 cyclic, thermomechanical tensile tests of programmed specimens (ε_{prog} = 350%) were performed in a thermochamber by repetitive heating and cooling from T_{low} = 25 °C to T_{high} = 90 °C (95 °C) under stress-free conditions (Experimental, Supporting Information). The results of these investigations are displayed in Figure 2 and Figure S5. To investigate the long-term

behavior of the noncontinuous actuator a multicycle experiment of around 140 cycles was performed. The dependence of strain on the number of cycles is shown in Figure 2a. A uniform reversible actuation was observed with stable nonresponding plateaus observed in all heating and cooling cycles. Identical performance was observed in all measurements indicating the long-term durability of the interruptive soft actuator. Substantial overall reversible elongation of $\Delta\varepsilon = 25\pm1\%$ was obtained, which is divided into two almost equal actuation contributions from the PCL and PE domains, interrupted by the stop in the nonresponse region. The final state at 90 °C is stabilized by remaining PE crystallites, thus the full recovery of the sample is restricted by the crystals present above T_{high}.

Commonly, crystallization of polymers is investigated under isothermal conditions close to the melting or crystallization temperature of the respective material. In this study non-isothermal cooling profiles are applied to the system to allow slow cooling, and subsequently to enable more uniform nucleation and crystal growth from the melt resulting in thick crystals. On the contrary fast cooling rates reduce the chain mobility and lead preferably to an increase of the number of small nuclei in the domains. As expected, by varying the heating/cooling rate, which is limited by the used thermochamber to rates between 0.5 to 10 K min^{-1} with a constant temperature increase/decrease (see Table S4), we observed differences in the actuation performance of our material. Polyethylene shows a constant and very fast crystallization in the investigated range[27]. Furthermore, remaining PE crystals ($T_{high} < T_{m,offset}$) act as seeds in the PE domain, increasing nucleation rates. In case of PCL, slow cooling rates promote PCL crystallization, while fast cooling induces small crystals, which lead to a decrease in the crystallinity (Table S3; DSC measurements with different cooling rates can be found in Figure S2) and changes in the response onset temperature (Figure 2c).[28-30] By decreasing the heating rate an increase in the onset temperature of the shape shift from 50 to 56 °C is observed (Figure 2b), which showed a linear correlation with the applied heating rate (Figure S6). The independence of polyethylene crystal melting is indicated by a perfect overlay of the determined shape shift. A similar trend is also observed for the reverse behavior. As the actuation mechanism is influenced by the crystallinity a decrease here leads to reduced actuation capability. To ensure higher degrees of crystallinity for PCL the measurements were repeated with lower $T_{low} = 10$ °C, a temperature well below the crystallization temperature of PCL (see Table S4), which did not lead to an improvement. For fast cooling rates PE related actuation remains the same as for slow cooling rates, while the hysteresis is more pronounced for the PCL induced elongation. The width of the nonresponse plateau changes dramatically and correlates strongly with the PCL melting, leading to the conclusion that the early melting of the PCL leads

to a broader nonresponse temperature interval. The actuation of the PCL domains is reduced with the thinner crystals obtained at faster cooling rates, reducing the material's expansion. A schematic representation of different crystallization behavior in co-continuous cPCL-PEVA upon fast or slow cooling is illustrated in Figure 2d. The thermal response of the material is connected with the crystallization/melting of the respective domain, which can be observed by DSC, where the melting of the domain can be translated into contraction and formation of crystals during cooling causing elongation (Δε, Figure S4).

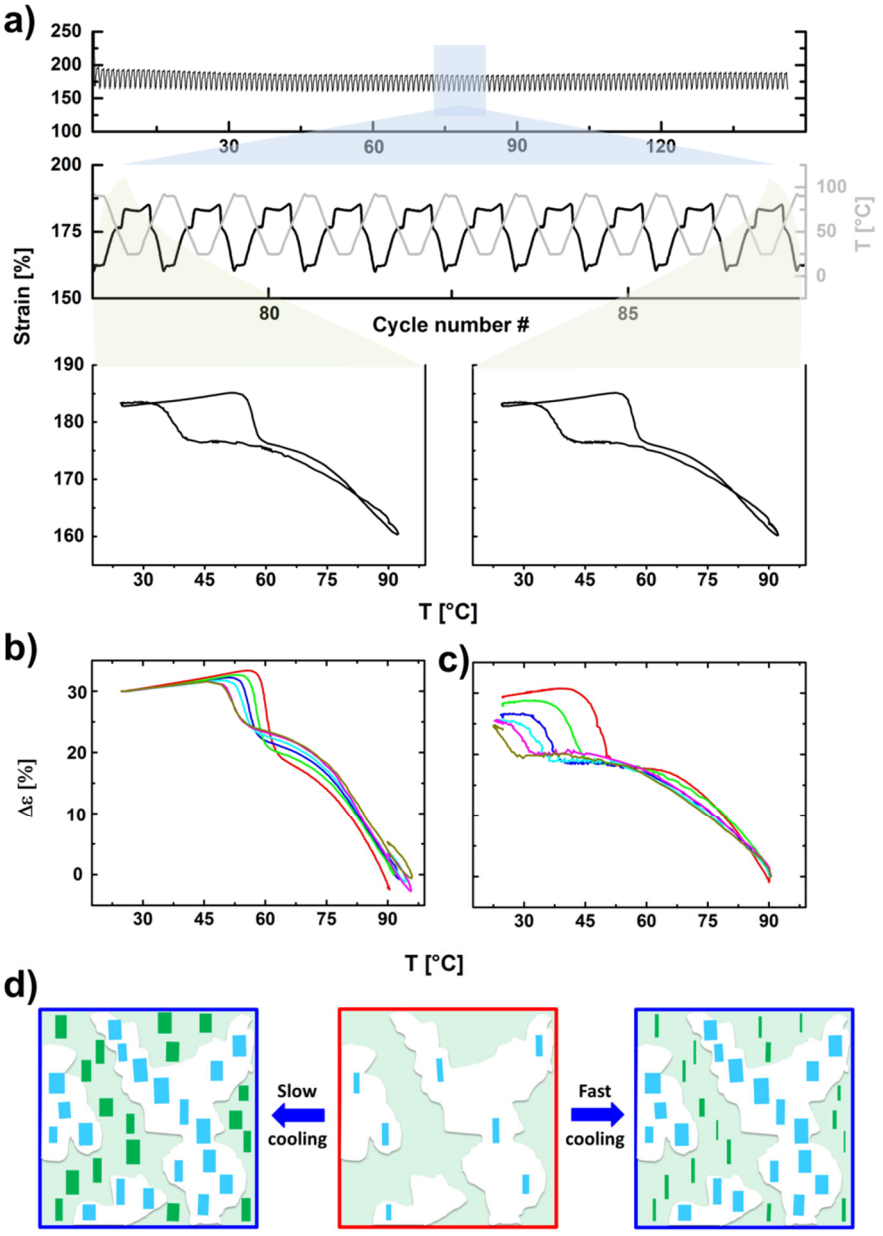

Figure 2: a) Multicyclic actuation test of cPCL-PEVA5 network with T_{prog} = 110 °C, ε_{prog} = 350%, T_{low} = 25 °C and T_{high} = 90 °C with heating and cooling rates of 3 K min^{-1}. **b)** Effect of heating rate 0.5 (red), 2 (green), 4 (blue), 6 (cyan), 7.6 (magenta) and 8.4 K·min^{-1} (dark yellow) and **c)** cooling rates 0.5 (red), 2 (green), 4 (blue), 6 (cyan), 8 (magenta) and 10 K·min^{-1} (dark yellow) on the actuation behavior. **d)** Schematic illustration of

crystallization of co-continuous blend network of PCL and PEVA from T_{high} (red) – slow cooling rates lead to a higher degree of crystallinity for PCL (green) in respective domains in comparison to fast cooling rates, while the PE (blue) crystallization is not influenced, resulting in reduced actuation performance only related to PCL domains.

Further characterization of the micro- and nano-morphological changes during actuation were performed by temperature-dependent AFM measurements (see Figure S7) and wide- and small-angle x-ray scattering measurements (WAXS and SAXS) as has been performed before for shape-memory actuators. From the results, we observe highly oriented crystalline domains confined within a matrix. The melting and crystallization of the respective domains in the measured temperature range correspond to the macroscopic movements of the material (for further details see Table S5, Figures S8). As these measurements were all performed as offline measurements the discontinuous behavior cannot be characterized by these methods.

The high processability and cost effectiveness of commodity polymers (such as PEVA and PCL) make them industrially viable for the creation of actuators displaying complex movements, which require more freedom in motion. Via this approach, we introduced non-continuous actuators showing characteristic nonresponse intervals during heating and cooling. Such noncontinuous performance are required in typical daily devices, which could also be used in almost autonomously working devices applying a constant trigger like for example for control traffic light or scrolling advertisement boards. A traffic lights and a advertising banner demonstrator were constructed based on a rotating wheel setup driven by programmed twisted cPCL-PEVA5 stripes. The interruptive actuation was examined by continuous cyclic heating and cooling between T_{low} = 25 °C to T_{high} 85 °C in a closed heating chamber. In Figure 3a and 3b respective image series taken from the videos (Supporting Information Videos S2 and S3) are displayed, where the centered yellow color documents the nonresponse temperature intervals. A more detailed analysis of the change in angle or length with temperature can be found in Figure S10 and S11. The nonresponse temperature ranges of all “twisted stripe”-driven demonstrators are in good agreement. Finally, the temperature dependent actuation behavior of a perpendiculary deformed originally flat cPCL-PEVA5 spiral was explored, whereby the overall change in spiral height (z-direction) was followed upon temperature alteration between 25 °C and 90 °C. Representative, photographs taken from Supporting Information Video S4 are shown in Figure 3c. Here the nonresponse range is characterized by the stop in height change while heating and cooling.

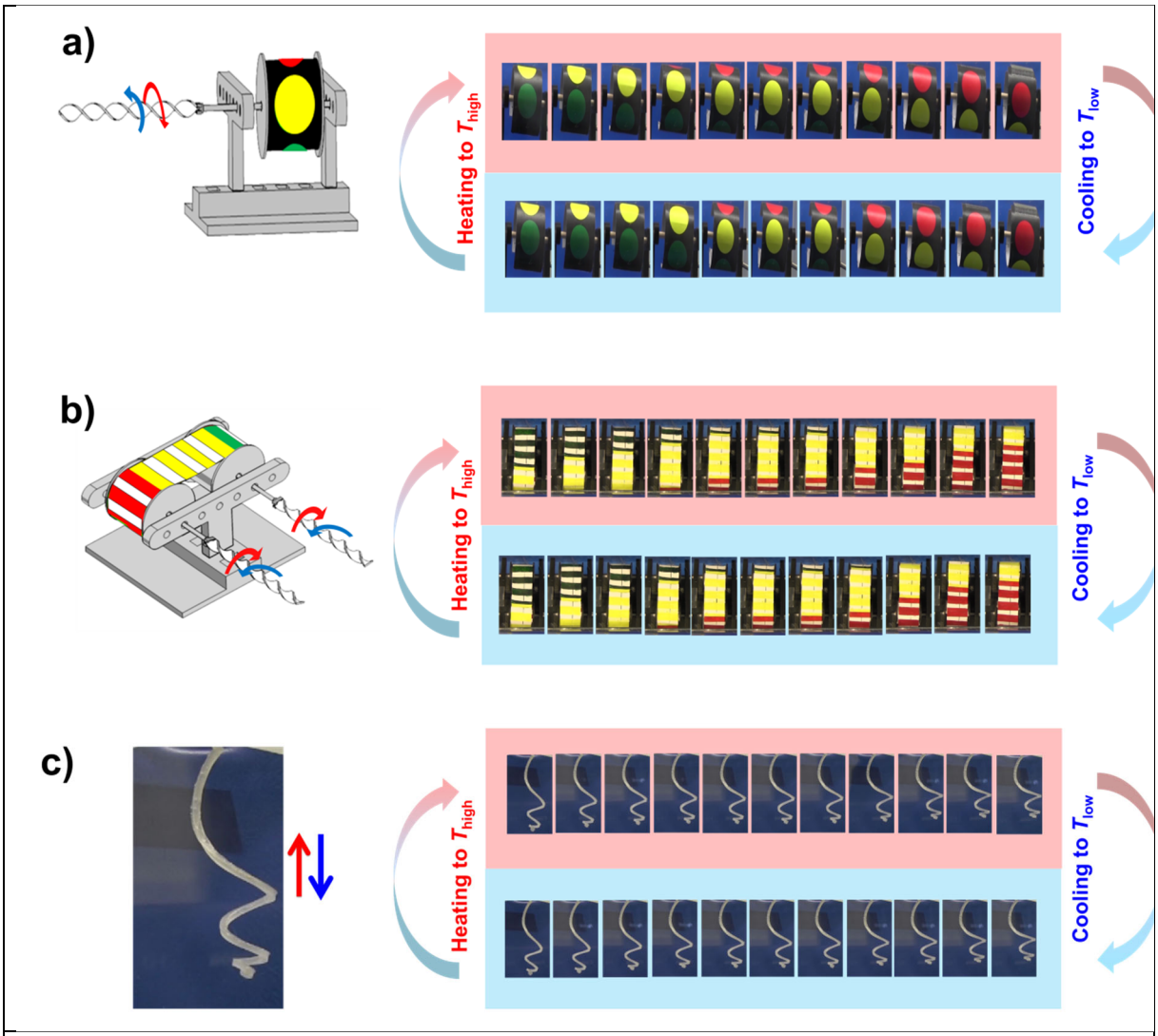

Figure 3: Picture series of second heating and cooling cycle demonstrating noncontinuous actuation in **a)** traffic light and **b)** advertising banner, both controlled by twisted cPCL-PEVA5 actuator stripes. **c)** Series of photographs showing the interruptive actuation of an extended actuator spiral.

In this study we have demonstrated interruptive actuators based on crosslinked co-continuous blends of PCL and PEVA. The noncontinuous movement described here, in which we can stop an actuation without an additional external trigger or antagonist, represents a new level of complexity in the movement of soft actuators. This behavior was explored further by investigating the influence of crystallization kinetics via variations of surface-to-volume ratio or heat transfer rates. Polymers with similar or even more complex crystallization behavior could be incorporated into such noncontinuous actuators, which might lead to even more sophisticated nonlinear response behavior during heating or cooling. By replacing the commercially available polymers used here with tailor-made materials, the current performance of 25% reversible shape shifts could potentially be improved, leading to a variety of new applications.

Supporting information

Methods, experiments and additional measurements/data are provided in the Supporting Information.

Acknowledgements

This work was supported by the Helmholtz-Association through program-oriented funding. The authors thank Susanne Schwanz and Richard Neumann for technical support and Oliver Gould for his fruitful discussion throughout the revisions.

References

1. Hines, L.; Petersen, K.; Lum, G. Z.; Sitti, M. Soft Actuators for Small-Scale Robotics *Adv. Mater.* **2017,** *29*, 1603483.
2. Ham, R. V.; Sugar, T. G.; Vanderborght, B.; Hollander, K. W.; Lefeber, D. Compliant Actuator Designs *IEEE Robotics & Automation Magazine* **2009,** *16*, 81-94.
3. Rus, D.; Tolley, M. T. Design, Fabrication and Control of Soft Robots *Nature* **2015,** *521*, 467-475.
4. Iida, F.; Laschi, C. Soft Robotics: Challenges and Perspectives *Procedia Comput. Sci.* **2011,** *7*, 99-102.
5. Bauer, S.; Bauer-Gogonea, S.; Graz, I.; Kaltenbrunner, M.; Keplinger, C.; Schwodiauer, R. 25th Anniversary Article: A Soft Future: From Robots and Sensor Skin to Energy Harvesters *Adv. Mater.* **2014,** *26*, 149-162.
6. Roche, E. T.; Wohlfarth, R.; Overvelde, J. T. B.; Vasilyev, N. V.; Pigula, F. A.; Mooney, D. J.; Bertoldi, K.; Walsh, C. J. A Bioinspired Soft Actuated Material *Adv. Mater.* **2014,** *26*, 1200-1206.
7. Wehner, M.; Truby, R. L.; Fitzgerald, D. J.; Mosadegh, B.; Whitesides, G. M.; Lewis, J. A.; Wood, R. J. An Integrated Design and Fabrication Strategy for Entirely Soft, Autonomous Robots *Nature* **2016,** *536*, 451-455.
8. Haines, C. S.; Li, N.; Spinks, G. M.; Aliev, A. E.; Di, J. T.; Baughman, R. H. New Twist on Artificial Muscles *Proc. Natl. Acad. Sci. U. S. A.* **2016,** *113*, 11709-11716.
9. Trimmer, B. Humanoids and the Emergence of Soft Robotics *Soft Robotics* **2015,** *2*, 129-130.
10. Koerner, H.; Price, G.; Pearce, N. A.; Alexander, M.; Vaia, R. A. Remotely Actuated Polymer Nanocomposites—Stress-Recovery of Carbon-Nanotube-Filled Thermoplastic Elastomers *Nat. Mater.* **2004,** *3*, 115-120.
11. Stoyanov, H.; Kollosche, M.; Risse, S.; Waché, R.; Kofod, G. Soft Conductive Elastomer Materials for Stretchable Electronics and Voltage Controlled Artificial Muscles *Adv. Mater.* **2013,** *25*, 578-583.
12. Habrard, F.; Patscheider, J.; Kovacs, G. Stretchable Metallic Electrodes for Electroactive Polymer Actuators *Adv. Eng. Mater.* **2014,** *16*, 1133-1139.
13. Meis, C.; Montazami, R.; Hashemi, N. Ionic Electroactive Polymer Actuators as Active Microfluidic Mixers *Anal. Methods* **2015,** *7*, 10217-10223.
14. Ohm, C.; Brehmer, M.; Zentel, R. Liquid Crystalline Elastomers as Actuators and Sensors *Adv. Mater.* **2010,** *22*, 3366-3387.
15. Jiang, H.; Li, C.; Huang, X. Actuators Based on Liquid Crystalline Elastomer Materials *Nanoscale* **2013,** *5*, 5225-5240.

16. Yang, Y.; Zhan, W.; Peng, R.; He, C.; Pang, X.; Shi, D.; Jiang, T.; Lin, Z. Graphene‐Enabled Superior and Tunable Photomechanical Actuation in Liquid Crystalline Elastomer Nanocomposites *Adv. Mater.* **2015,** *27*, 6376-6381.
17. Ube, T.; Ikeda, T. Photomobile Polymer Materials with Crosslinked Liquid‐Crystalline Structures: Molecular Design, Fabrication, and Functions *Angew. Chem., Int. Ed.* **2014,** *53*, 10290-10299.
18. Bothe, M.; Pretsch, T. Bidirectional Actuation of a Thermoplastic Polyurethane Elastomer *J. Mater. Chem. A* **2013,** *1*, 14491-14497.
19. Gong, T.; Zhao, K.; Wang, W.; Chen, H.; Wang, L.; Zhou, S. Thermally Activated Reversible Shape Switch of Polymer Particles *J. Mater. Chem. B* **2014,** *2*, 6855-6866.
20. Pandini, S.; Passera, S.; Messori, M.; Paderni, K.; Toselli, M.; Gianoncelli, A.; Bontempi, E.; Ricco, T. Two-Way Reversible Shape Memory Behaviour of Crosslinked Poly(E-Caprolactone) *Polymer* **2012,** *53*, 1915-1924.
21. Behl, M.; Kratz, K.; Nöchel, U.; Sauter, T.; Lendlein, A. Temperature-Memory Polymer Actuators *Proc. Natl. Acad. Sci. U. S. A.* **2013,** *110*, 12555-12559.
22. Volkov, A. G.; Carrell, H.; Baldwin, A.; Markin, V. S. Electrical Memory in Venus Flytrap *Bioelectrochemistry* **2009,** *75*, 142-147.
23. Volkov, A. G.; Harris, S. L., 2nd; Vilfranc, C. L.; Murphy, V. A.; Wooten, J. D.; Paulicin, H.; Volkova, M. I.; Markin, V. S. Venus Flytrap Biomechanics: Forces in the Dionaea Muscipula Trap *J. Plant Physiol.* **2013,** *170*, 25-32.
24. Volkov, A. G.; Pinnock, M. R.; Lowe, D. C.; Gay, M. S.; Markin, V. S. Complete Hunting Cycle of Dionaea Muscipula: Consecutive Steps and Their Electrical Properties *J. Plant Physiol.* **2011,** *168*, 109-120.
25. Pandini, S.; Dioni, D.; Paderni, K.; Messori, M.; Toselli, M.; Bontempi, E.; Ricco, T. The Two-Way Shape Memory Behaviour of Crosslinked Poly(Epsilon-Caprolactone) Systems with Largely Varied Network Density *J. Intell. Mater. Syst. Struct.* **2016,** *27*, 1388-1403.
26. Arnebold, A.; Hartwig, A. Fast Switchable, Epoxy Based Shape-Memory Polymers with High Strength and Toughness *Polymer* **2016,** *83*, 40-49.
27. Supahol, P.; Spruiell, J. E. Nonisothermal Bulk Crystallization Studies of High Density Polyethylene Using Light Depolarizing Microscopy *J. Polym. Sci., Part B: Polym. Phys.* **1998,** *36*, 681-692.
28. Zhuravlev, E.; Schmelzer, J. W. P.; Wunderlich, B.; Schick, C. Kinetics of Nucleation and Crystallization in Poly(Ɛ-Caprolactone) (PCL) *Polymer* **2011,** *52*, 1983-1997.
29. Lorenzo, M. L. D.; Silvestre, C. Non-Isothermal Crystallization of Polymers *Prog. Polym. Sci.* **1999,** *24*, 917-950.
30. Skoglund, P.; Fransson, A. Continuous Cooling and Isothermal Crystallization of Polycaprolactone *J. Appl. Polym. Sci.* **1996,** *61*, 2455-2465.

Graphic for manuscript